Scientific report; WR 2005-03

KNMI

On the role of the vertical velocity profile in the tropical tropopause on cold point formation

Peter Siegmund

De Bilt, 2005

Scientific report = wetenschappelijk rapport; WR 2005-03

De Bilt, 2005

PO Box 201
3730 AE De Bilt
Wilhelminalaan 10
De Bilt
The Netherlands
http://www.knmi.nl
Telephone +31(0)30-220 69 11
Telefax +31(0)30-221 04 07

Author: Siegmund, P.

On the role of the vertical velocity profile in the tropical tropopause layer on cold point formation

Peter Siegmund

Royal Netherlands Meteorological Institute (KNMI), De Bilt, The Netherlands

Abstract

The effect of the observed decrease of the vertical velocity with height in the tropical tropopause layer on the formation of the cold point has been investigated, using a very simple model of the approximate balance between vertical temperature advection and radiative heating. The modeled large-scale and monthly-mean temperature profile has a cold point not only if the radiative equilibrium temperature increases with height, which is the usual explanation for the cold point, but also if the vertical velocity decreases with height. If in the model the vertical velocity is assumed to decrease with height as observed, and other parameters, particularly the radiative equilibrium temperature, are fixed, then the modeled cold point height and temperature are close to the observations. This suggests that the observed decrease of the vertical velocity with height in the tropical tropopause layer plays an important role in the formation of the cold point.

1. Introduction

The processes that determine the tropical cold point tropopause are not fully understood [e.g., *Highwood and Hoskins,* 1998; *Kuang and Bretherton*, 2004]. Recently it has become clear that the cold point does not coincide with the top of the convection, but is situated several km above it [e.g., *Folkins et al.*, 1999; *Gettelman et al.*, 2002]. Thus, radiative processes, rather than latent heat release, are expected to be relevant for the formation of the cold point. The layer between the level of main convective outflow and the cold point tropopause is commonly called the Tropical Tropopause Layer (TTL) [*Gettelman and Forster*, 2002].

In the TTL an approximate balance exists between the vertical temperature advection and radiative heating [e.g., *Corti et al.*, 2005]:

$$w\left(\frac{\partial T}{\partial z}+\frac{g}{c_p}\right)=\frac{T_{rad}-T}{\tau}, \qquad (1)$$

where w is the vertical velocity, T is temperature, z is height, and g/c_p is the dry adiabatic lapse rate. The radiative heating in Eq. (1) is approximated by a relaxation with time scale τ towards the radiative equilibrium temperature T_{rad} [*Newman and Rosenfield,* 1997]. Solutions $T(z)$ of Eq. (1) have a cold point if T_{rad} increases with height (see Section 2). This is the usual explanation for the existence of a cold point, where the increase of T_{rad} with height is explained by the increase with height of the absorption of solar radiation by ozone. However, solutions of Eq. (1) also have a cold point if $w\tau$ *decreases* with height (see Section 2). Several studies indicate that in the TTL the zonal- and time mean (upward) vertical velocity indeed decreases with height [*Rosenlof,* 1995; *Dunkerton,* 1997; *Corti et al.* 2005], whereas τ in this region is relatively constant [*Newman and Rosenfield*, 1997]. This suggest that the decrease with height of the vertical velocity in the TTL might be relevant for the formation of the cold point.

Here we investigate whether this is indeed the case. Solutions $T(z)$ of Eq. (1) will be considered, using the mentioned estimates of $w(z)$ in the TTL, and keeping the other

parameters, particularly T_{rad}, fixed. The computed $T(z)$ is compared with observations. The results show that the computed cold point is close to the observations, indicating that the vertical wind profile in the TTL is a main factor in the formation of the cold point.

2. Temperature profile solutions of Eq. (1)

Equation (1) can be solved easily in several simplified cases. Let us first assume that T_{rad} increases linearly with z, i.e. $T_{rad}=T_{rad,0}+az$, with $a>0$, and that w and τ are independent of z. From Eq. (1) it follows directly that $T_{rad,0}=T_0+w\tau(T_{z0}+g/c_p)$, where T_0 and T_{z0} are, respectively, the temperature and the lapse rate at $z=0$. The level $z=0$ is in the TTL, below the cold point, and hence T_{z0} is negative. The solution of Eq. (1) is

$$T(z) = T_0 + az - w\tau(a - T_{z0})(1 - \exp(-z/w\tau)). \tag{2}$$

If $a>0$ then $T(z)$ has a cold point ($\partial T/\partial z=0$), with a height z_{cp} and temperature T_{cp} equal to

$$z_{cp} = w\tau \ln(1 - \frac{T_{z0}}{a}), \text{ and} \tag{3a}$$

$$T_{cp} = T_0 + w\tau T_{z0} + a\, z_{cp}. \tag{3b}$$

To analyse $T(z)$, it is convenient to define the scaled quantities $T^* \equiv T/(gw\,\tau/c_p)$, $z^* \equiv z/(w\tau)$, and $a^* \equiv a/(g/c_p)$. The profile $T^*(z^*)$ is shown in Fig. 1 (thin lines) for different values of a^*, adopting $T_0=0$ and $T_{z0}=-g/c_p$. With increasing a^*, the z^*_{cp} decreases and T^*_{cp} increases. If $a^*=0$ (dash-dot line), then $Z^*_{cp}=\infty$ and $T^*_{cp}=-1$.

Next consider the simplified case that w decreases linearly with z, i.e. $w=w_0+bz$, with $b<0$, and that T_{rad} and τ are independent of z. Then

$$T(z) = T_0 + w_0\tau(T_{z0} + \frac{g}{c_p})(1 - (1 + \frac{bz}{w_0})^{-1/b\tau}) - \frac{w_0\tau g}{c_p(1+b\tau)}((1 + \frac{bz}{w_0}) - (1 + \frac{bz}{w_0})^{-1/b\tau}). \tag{4}$$

If $b<0$ this $T(z)$ has a cold point, with z_{cp} and T_{cp} equal to

$$z_{cp} = \frac{-w_0}{b}\left[1-\left(1+\frac{c_p T_{z0}}{g}\frac{(1+b\tau)}{b\tau}\right)^{\frac{b\tau}{1+b\tau}}\right], \text{ and} \tag{5a}$$

$$T_{cp} = T_0 + w_0\tau T_{z0} - b\tau\, z_{cp}\, g/c_p. \tag{5b}$$

The profile $T^*(z^*)$ for different values of $b^* \equiv b\tau$ is shown in Fig. 1 (thick lines), adopting $T_0=0$ and $T_{z0}=-g/c_p$, and defining $T^* \equiv T/(g w_0 \tau/c_p)$, and $z^* \equiv z/(w_0\tau)$. With decreasing b^*, the z^*_{cp} decreases and T^*_{cp} increases. If $b^*=0$ (dash-dot line), then $Z^*_{cp}=\infty$ and $T^*_{cp}=-1$. At $z^*=-1/b^*$, the vertical velocity is zero. Above this level, where the ascending air does not arrive, the model has no solution.

3. Application to the TTL

3.1. The vertical velocity profile

The studies of *Rosenlof* [1995] and *Corti et al.* [2005] indicate that in the TTL the zonal- and time-mean vertical velocity decreases with height. Rosenlof's vertical velocity values between 15 and 19 km for January and July 1992-1994 are shown in Fig. 2 (solid lines). She computed the transformed Eulerian-mean vertical velocity (w^*), using a radiative model together with temperature and constituent data. The values of w^* are averages within 10° of the equator, and are shown by Dunkerton [1997, Figure 7]. *Corti et al.* computed the annual mean vertical mass flux in the equatorial belt, using a radiative model together with cloud data. From this mass flux we computed the vertical velocity (w), shown by the dashed line in Fig. 2, by dividing it by the air mass density, using typical values for the tropical atmosphere [*McClatchey et al.*, 1972]. Rosenlof's 'annual'-(January plus July) mean values are somewhat larger than those of *Corti et al.* This might be due to the difference between w^* and w, and to differences in the radiative models and input data. The latter differences are probably dominating, as in the tropics the eddy heat flux divergence, which determines the difference between w and w^*, is small [e.g., *Peixoto and Oort*, 1992]. Also shown in Fig. 2 is the vertical velocity for January and July 1992-1994,

averaged within 10° of the equator, as derived from European Centre for Medium-Range Weather Forecasts (ECMWF) operational first guess-data. This vertical velocity is computed from the divergence of the horizontal wind. As in the other profiles in Fig. 2, its value in the TTL decreases with height. Its values are about half as large as those computed by Rosenlof. This difference is probably due to the difference in the methods to compute the vertical velocity. We expect Rosenlof's values to be more realistic, as they are closer to the values independently derived from the ascent rate of water vapour anomalies by *Mote et al.* [1996]. Therefore, we will tentatively use Rosenlof's estimates of the vertical velocity.

3.2. The observed temperature profile

The 'observed' large-scale temperature profiles in January and July are shown in Fig. 3. They have been derived from ECMWF temperature analyses, with a horizontal resolution of 2.5° and a vertical resolution of about 1 km. They are, like the vertical velocity, mean values for 1992-1994, averaged within 10° of the equator. Hereafter this temperature will be called the observed temperature. In the computation of $T(z)$ with Eq. (4), z_0 (the height of z=0) is at the ECMWF model level nearest to 16 km. Both in January and July z_0=15.93 km. At this level the temperature, T_0, is 194.71 K in January and 196.29 K in July. As z_0 is chosen to be a model level, there is no interpolation error in T_0. The z_0 is below the cold point (see below) and above the convection top [*Folkins et al.*, 1999], and is therefore a suitable lower boundary for application of Eq. (4). The T_{z0} is computed as the first derivative in z_0 of the quadratic polynomial that fits the observed temperature profile at z_0 and at the two levels above and below this level (for January this is the fit through points 1, 2, and 3 in Fig. 3). Its value is –4.24 K km^{-1} in January and –1.95 K km^{-1} in July. However, these values likely contain errors due to the limited vertical resolution of the data. The value of T_{z0} in January is estimated between –5.60 and –2.72 K km^{-1}, which are the slopes of the line segments 1-2 and 2-3 in Fig. 3. For July the corresponding range of T_{z0} is from –4.74 to +0.90 K km^{-1}.

The cold point is calculated as the minimum of the quadratic polynomial that fits the observed temperature profile at the level with the lowest temperature and the two levels below and above this level (for January this is the fit through points 2, 3, and 4 in Fig. 3). The cold point height and temperature, indicated by a plus-sign in Fig. 3, are 17.06 km and 191.56 K in January, and 16.33 km and 195.89 K in July.

However, these values likely contain errors due to the limited vertical resolution of the data. The real cold point is expected to be within the triangular, shaded regions in Fig. 3, hereafter called the cold point region. These are the regions where the cold point can exist if the temperature profile fits the points 1 through 5, and if it is assumed that between these points the lapse rate increases with increasing height (see Fig. 3). There is one triangular region left and one right of point 3. The left triangle is formed by the lines 1-2, 3-4, and the horizontal line through point 3. The right triangle is formed by the latter line, and the lines 5-4 and 2-3.

3.3. The modeled temperature profile

We will now compute the temperature profile that follows from Eq. (4) for January and July, using the observed values of the different variables as mentioned above, and compare it with the observed profile.

For January we use w_0=0.92 mm s^{-1} and b= –0.25 mm s^{-1} km^{-1}. Between 16 and 18 km this linear profile is a good approximation of the result of *Rosenlof* [1995] shown in Fig 2. The value of τ in the TTL varies between about 25 and 30 days [*Newman and Rosenfield*, 1997]. We assume a value of 30 days, which was also assumed by *Yulaeva et al.* [1994]. As follows from Eq. (1), it are the vertical variations in the product $w\tau$ rather than in w that are relevant for the temperature profile. However, in the TTL $w(z)$ varies by more than 100%, whereas $\tau(z)$ varies only about 20%. Therefore, in first approximation, we neglect vertical variations in τ. With g=9.81 ms^{-2} and c_p=1004 J $kg^{-1}K^{-1}$, all parameters in Eq. (4) have now assigned a value, allowing the computation of $T(z)$. The modeled $T(z)$ is shown in Fig. 4a (solid line). The modeled cold point is indicated by a cross. The observed temperature profile is indicated by the dotted line, and its estimated cold point and cold point region are indicated by the plus-sign and the shaded region, respectively. Fig. 4a shows that between about 16 and 18 km, where the adopted linear vertical velocity profile is valid, there exists a good agreement between the observed temperature profile and the profile from our simple model. The differences between the modeled and observed cold point height and temperature (model minus observed) are 0.06 km and 0.56 K, respectively. Although the modeled cold point height is close to the observed value, the modeled cold point temperature is not within the estimated observed cold point region. If T_{z0}, which is –4.24 K km^{-1} for the solid line in Fig. 4a, is decreased to –4.8 K km^{-1}, which is within the estimated range of T_{z0}, then the

temperature profile (dashed line in Fig. 4a) has a cold point within the observed cold point region. As described in Section 2, the existence of a cold point in $T(z)$ of Eq. (4) is due solely to the decrease of the vertical velocity with height. The close correspondence between the modeled and observed cold point indicates, that the decrease of the vertical velocity with height is a main factor in the formation of the cold point. In particular, this shows that there is *no* need for an increase of T_{rad} with height to simulate a realistic cold point. Adding an increase of T_{rad} with height to the model would even deteriorate the result, as this would increase the modeled cold point temperature, which already tends to be too large.

For July we use w_0=0.51 mm s^{-1} and b= –0.2 mm s^{-1} km^{-1}, as derived from Rosenlof's profile for July in Fig. 2. As shown in Fig. 4b, there exists between about 16 and 17 km a good correspondence between the modeled (solid line) and observed (dotted line) temperature profile. The modeled cold point height and temperature are within the observed cold point region. Their differences with the observed cold point are 0.03 km and –0.02 K, respectively. Although these differences are small, this is perhaps not very surprising, since z_0 is taken very close to the observed cold point. Therefore, we also computed a temperature profile taking z_0 one ECWMF model level below that in the previous computations, which is at 14.89 km. At this level T_0=200.95 K, w_0=0.83 mm s^{-1}, b= –0.25 mm s^{-1} km^{-1}, T_{z0}=–5.45 K km^{-1}, and the range of T_{z0} is from –6.36 to –4.47 K km^{-1}. This modeled temperature profile is shown by the dashed line in Fig. 4b. Although the modeled cold point height is within the observed cold point region, the modeled cold point temperature is about 1 K too high. If T_{z0} is decreased to the lower value of its estimated range, then the modeled cold point temperature (dash-dotted line in Fig. 4b) is just within the cold point region. We conclude that also in July the decrease of the vertical velocity with height in the TTL is a main factor in the formation of the cold point.

3.4. The modeled temperature profile above the cold point

Given the results of Section 3.3, the question arises to what extent Eq. (1) can simulate the temperature profile *above* the cold point, if all parameters are fixed, except the vertical velocity. We have integrated Eq. (1) numerically to a height of 24 km, using the vertical velocity profiles of Rosenlof and keeping all other parameters fixed. For z_0, T_0, T_{z0}, and τ, the same values were used as those for the dashed line in Fig. 4a for January and the dash-dotted line in Fig. 4b for July, for which the cold

points are close to the observations. As shown in Fig. 5, above the cold point the observed lapse rate is positive, but the simulated lapse rate above about 20 km is negative. Both in January and July, up to about 2 km above the cold point the modeled and observed lapse rates have similar values, indicating that here the decrease of the vertical velocity with height is a main factor determining the observed temperature profile. Above this higher level likely the increase of T_{rad} with height mainly explains the observed temperature profile.

4. Conclusion

We have argued that at large spatial and temporal scales the observed decrease of the vertical velocity with height in the TTL likely plays a major role in the formation of the cold point tropopause. In particular, in the simple but essentially correct model of Eq. (1) there is no need for an increase of the radiative equilibrium temperature with height to simulate the observed cold point adequately.

Acknowledgments. The author would like to thank Peter van Velthoven and Paul Fortuin for their discussions and comments.

References

Corti, T., B. P. Luo, T. Peter, H. Vömel, and Q. Fu (2005), Mean radiative energy balance and vertical mass fluxes in the equatorial upper troposphere and lower stratosphere, *Geophys. Res. Lett., 32,* L06802, doi:10.1029/2004GL021889.

Dunkerton, T.J. (1997), The role of gravity waves in the quasi-biennial oscillation, *J. Geophys. Res., 102,* 26,053-26,076.

Folkins, I., M. Loewenstein, J. Podolske, S. Oltmans, and M. Proffitt (1999), A barrier to vertical mixing at 14 km in the tropics: Evidence from ozonesondes and aircraft measurements, *J. Geophys. Res., 104,* 22,095-22,102.

Gettelman A., M. L. Salby, and F. Sassi (2002), Distribution and influence of convection in the tropical tropopause region, *J. Geophys. Res., 107* (D10), doi:10.1029/2001JD001048.

Gettelman, A., and P. M. de F. Forster (2002), A climatology of the tropical tropopause layer, *J. Meteorol. Soc. Jpn., 80,* 911-924.

Highwood, E. J. and B. J. Hoskins (1998), The tropical tropopause, *Q. J. R. Meteorol. Soc., 124,* 1579-1604.

Kuang, Z., and C. S. Bretherton (2004), Convective influence on the heat balance of the tropical tropopause layer: A cloud-resolving model study. *J. Atmos. Sci., 61,* 2919-2927.

McClatchey, R. A., R., W., Fenn, J. E. A. Selby, F. E. Voltz and J. S. Garing, (1972), Optical properties of the atmosphere. 3d ed. AFCRL-72-0497, 108 pp. (NTIS-AD753075).

Mote, P. W., K. H. Rosenlof, M. E. McIntyre, E. S. Carr, J. C. Gille, J. R. Holton, J. S. Kinnersley, H. C. Pumphrey, J. M. Russell III, and J. W. Waters (1996), An

atmospheric tape recorder: The imprint of tropical tropopause temperatures on stratospheric water vapor, *J. Geophys. Res., 101,* 3989-4006.

Newman, P. and J. Rosenfield (1997), Stratospheric thermal damping times, *Geophys. Res. Lett., 24,* 433-436.

Peixoto, J. P., and A. H. Oort (1992), *Physics of Climate*, 520 pp., American Institute of Physics, New York.

Rosenlof, K. H. (1995), Seasonal cycle of the residual mean meridional circulation in the stratosphere, *J. Geophys. Res., 100,* 5173-5191.

Yulaeva, E., J. R. Holton, and J. M. Wallace (1994), On the cause of the annual cycle in the tropical lower stratospheric temperature, *J. Atmos. Sci., 51,* 169-174.

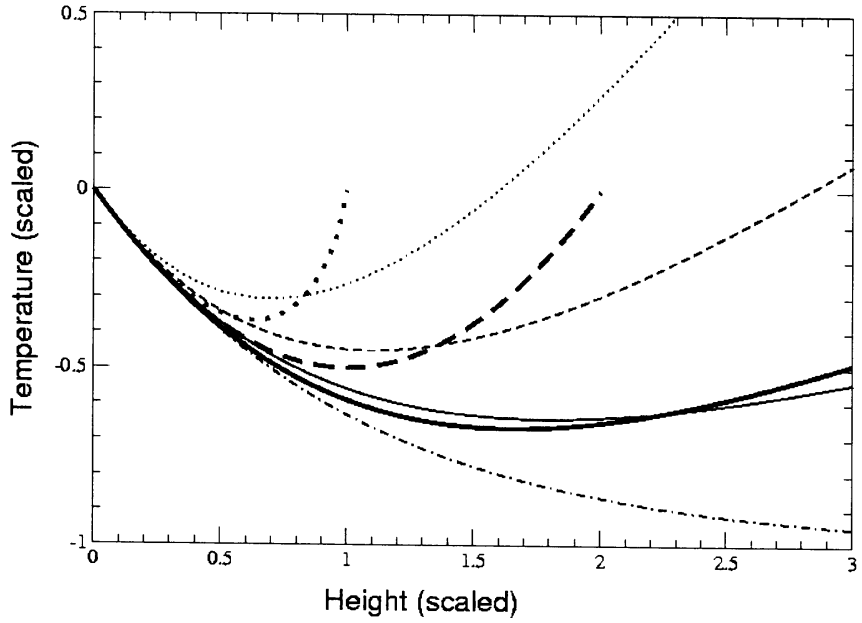

Figure 1. Profiles of $T^*(z^*)$ for a^* (thin lines) and $-b^*$ (thick lines) =0.2 (solid), 0.5 (dashed) and 1.0 (dotted), and for a^*=0 and b^*=0 (dash-dot). T^* and z^* are a scaled temperature and height, respectively. For their definition, and those of a^* and b^*, see the main text.

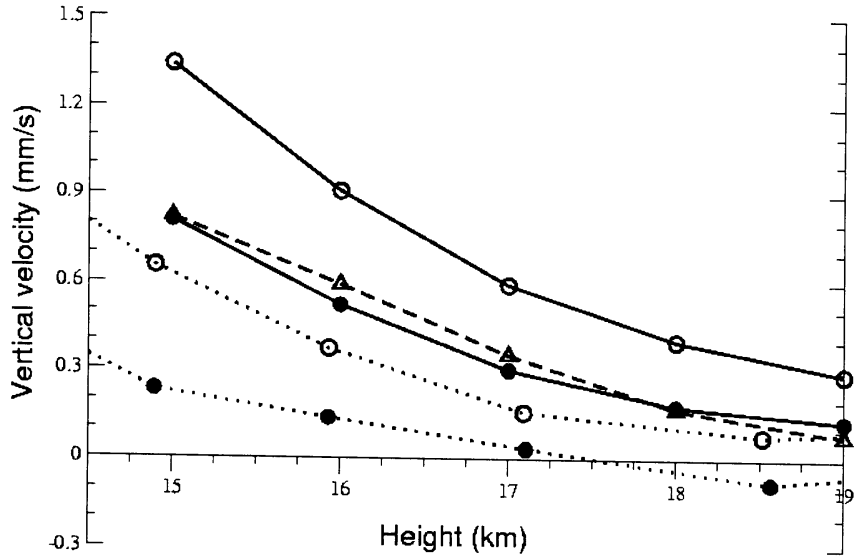

Figure 2. The vertical velocity (mm s^{-1}) as a function of height (km) in the TTL, as estimated with a radiative model by Rosenlof (1995) (solid lines, ○ is January, ● is July) and by Corti *et al.* (2005) (dashed line), and as represented by ECMWF first-guess data for 1992-1994 (dotted lines, ○ is January, ● is July).

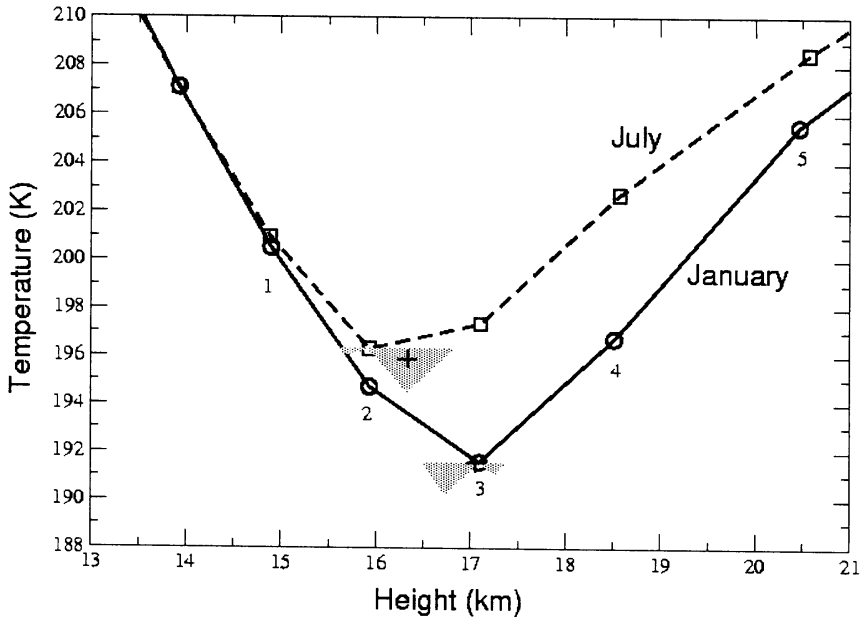

Figure 3. Temperature (K) as a function of height (km) in the TTL in January (solid line) and July (dashed line) 1992-1994, derived from ECMWF analyses. The + signs and the shaded regions indicate the estimated cold points and cold point regions, respectively (for their definitions see the main text).

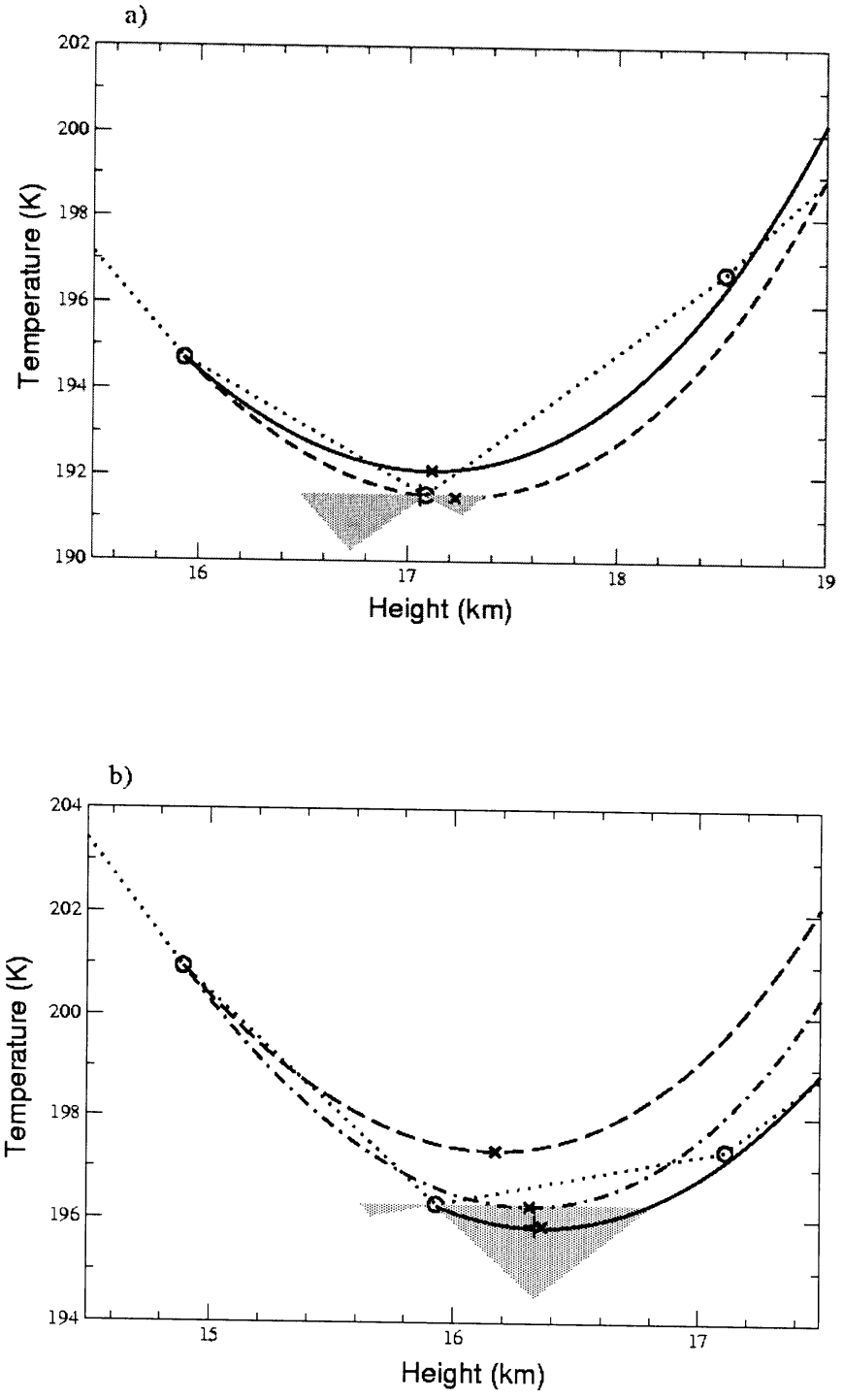

Figure 4. Temperature (K) as a function of height (km) in a) January and b) July, computed with Eq. (4), for different sets of parameters (see main text). The observed temperature profile is shown by the dotted lines. The × signs indicate the modeled cold points, the + sign and the shaded regions indicate the observed cold points and cold point region, respectively.

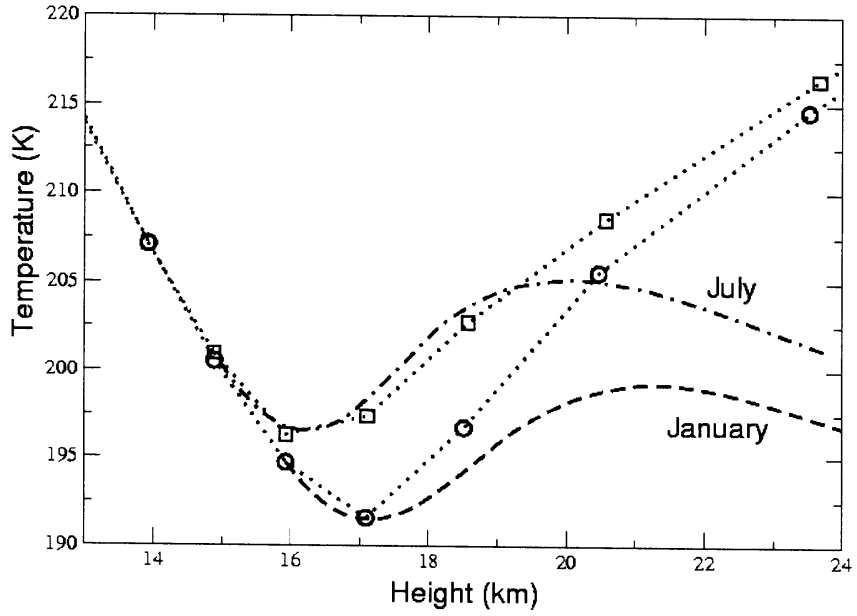

Figure 5. Temperature (K) as a function of height (km) in the TTL in January (dashed line) and July (dash-dot line), computed by numerically integrating Eq. (1), using the observed vertical velocity profile, and keeping all other parameters fixed. The dotted lines indicate the temperature derived from ECMWF analyses.